

# High-differential-quantum-efficiency, long-wavelength vertical-cavity lasers using five-stage bipolar-cascade active regions

R. Koda<sup>a)</sup> and C. S. Wang

Department of Electrical and Computer Engineering, University of California, Santa Barbara, California 93106

D. D. Lofgreen

Raytheon Vision Systems, Goleta, California 93117

L. A. Coldren

Department of Electrical and Computer Engineering, University of California, Santa Barbara, California 93106

(Received 15 October 2004; accepted 6 April 2005; published online 16 May 2005)

We present five-stage bipolar-cascade vertical-cavity surface-emitting lasers emitting at  $1.54\ \mu\text{m}$  grown monolithically on an InP substrate by molecular beam epitaxy. A differential quantum efficiency of 120%, was measured with a threshold current density of  $767\ \text{A}/\text{cm}^2$  and voltage of  $4.49\ \text{V}$ , only  $0.5\ \text{V}$  larger than  $5 \times 0.8\ \text{V}$ , the aggregate photon energy. Diffraction loss study on deeply etched pillars indicates that diffraction loss is a major loss mechanism for such multiple-active region devices larger than  $20\ \mu\text{m}$ . We also report a model on the relationship of diffraction loss to the number of active stages. © 2005 American Institute of Physics. [DOI: 10.1063/1.1931060]

Long-wavelength vertical-cavity surface-emitting lasers (VCSELs) are a promising low cost alternative to conventional edge-emitting lasers as transmitters for optical communication networks. Several different material systems have been investigated for  $1.55\ \mu\text{m}$  VCSELs with viable results by researchers. These include GaAs-based wafer fusion,<sup>1</sup> AlGaAsSb,<sup>2</sup> InP/air-gap distributed Bragg reflector (DBR),<sup>3</sup> and metamorphic DBR.<sup>4</sup> While all of them have high index contrast in DBRs, desirable for VCSELs, difficulties in growth or fabrication exist. An alternative choice is to use the AlInGaAs material system for the mirrors. This is an attractive material since the growth of AlInGaAs on InP is more mature than other material systems, such as AlGaAsSb. The main problem in this material is that the index contrast of the DBRs is relatively low. However, cascading active regions can more than compensate for this problem since a higher gain is possible by recycling of carriers.

Bipolar cascaded active region devices, also known as multiple-active-region (MAR) lasers, can be constructed by epitaxially stacking each stage of the active region in series with Esaki tunnel junctions.<sup>5</sup> A band diagram of a three-stage MAR is shown in Fig. 1. In MAR devices, carriers can be recycled through tunneling Esaki junctions, and as a result, a single electron entering the terminal can provide multiple photons, leading to uniform pumping and higher gain without the penalty of high bias current. Highly doped Esaki junctions can be placed at the null of the standing wave to minimize absorption loss.

Furthermore, bipolar-cascade VCSELs are attractive candidates for transmitters in optical networks where high differential efficiency and low-noise lasers are desirable. High efficiency is possible through the use of lower reflective DBRs<sup>6</sup> and higher signal to noise ratio is expected since

the signal is enhanced for the same noise when the active is divided into several stages.<sup>7</sup>

We have previously reported InP-based three-stage bipolar-cascade VCSELs with 94% differential quantum efficiency ( $\eta_d$ ) at  $-10\ ^\circ\text{C}$ .<sup>5</sup> Threshold voltage was  $3.3\ \text{V}$  which was only  $0.9\ \text{V}$  higher than the combined active junction voltages of  $2.4\ \text{V}$ . Although relatively successful, further optimization of growth and fabrication process was carried out to reduce the voltage drop across the DBRs and tunnel junctions (TJs). These involve band-gap engineering of the DBR interfaces as well as growth optimization for TJs. Air-post VCSELs presented previously are known to suffer from significant diffraction loss since the bottom DBRs possess no waveguiding.<sup>8</sup> An aperture can effectively eliminate such diffraction loss if designed properly, such as tapered oxide apertures used in a GaAs system.<sup>9</sup> The tapered aperture has a graded index, and thus can act as a lens to refocus a reflected mode reducing diffraction loss. However, the development of apertures in long-wavelength VCSELs with a single-growth monolithic approach has been difficult. While aperturing technologies have been developed by several research groups, for example using air gaps<sup>2</sup> or buried TJ apertures,<sup>10</sup> such elements are not very effective in multimode high-power applications where broad area devices are required.<sup>11</sup>

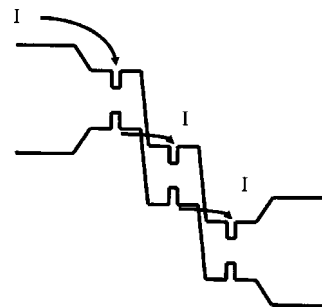


FIG. 1. Illustration of current path in bipolar-cascade lasers.

<sup>a)</sup>Electronic mail: rintaro@engineering.ucsb.edu

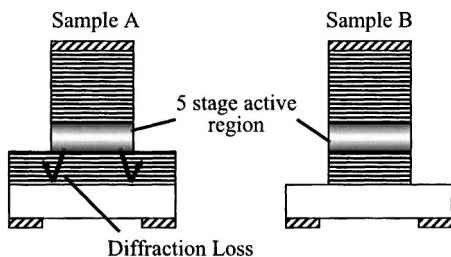


FIG. 2. Schematics of shallow (Sample A) and deeply etched (Sample B) pillars, illustrating diffraction loss from the bottom DBR for Sample A.

In these cases, diffraction loss of the higher-order modes appears to be a limiting factor. In this letter, we present a diffraction loss study of five-stage cascade VCSELs which have record differential efficiencies  $\sim 120\%$  and improved low-voltage DBRs and TJs, in which the excess voltage was only 0.5 V higher than the sum of the band-gap energies of 4 V.

A bottom-emitting  $1.55\ \mu\text{m}$  VCSEL structure with five-stage MAR was monolithically grown by molecular-beam epitaxy on an  $n$ -InP substrate. Top and bottom DBRs consisted of  $\text{Al}_{0.09}\text{In}_{0.53}\text{Ga}_{0.38}\text{As}/\text{Al}_{0.48}\text{In}_{0.52}\text{As}$  with a reflectivity of 99.8% and 98.3%, respectively. The interfaces of each DBR layer were graded over 32 nm to minimize conduction-band discontinuity. Each stage of the active region contained five 7 nm compressively strained quantum wells (QWs) ( $\text{Al}_{0.17}\text{In}_{0.67}\text{Ga}_{0.16}\text{As}$ ) and six 5 nm tensile strained barriers ( $\text{Al}_{0.20}\text{In}_{0.40}\text{Ga}_{0.40}\text{As}$ ). A 15 nm thick  $\text{Al}_{0.29}\text{In}_{0.52}\text{Ga}_{0.19}\text{As}$  TJ separated each stage and consisted of a 9 nm layer of Si doped  $n$ -type to  $5 \times 10^{19}\ \text{cm}^{-3}$  and a 6 nm layer of C doped  $p$ -type to  $2 \times 10^{20}\ \text{cm}^{-3}$ .

The structure was fabricated as air-post VCSELs where pillars were formed by an inductively coupled plasma etcher at  $200\ ^\circ\text{C}$ . As mentioned before, such a structure would suffer from diffraction loss through the bottom DBRs since no waveguiding is present. The diffraction loss of unguided DBRs is strongly dependent on the index contrast of the two DBR layers because the effective propagation distance is larger for a smaller contrast.<sup>8</sup> To study the effect, we have fabricated two samples: One where the pillar was etched through the active region (Sample A) and the other etched through the bottom DBR (Sample B) as shown in Fig. 2. Index guiding by the bottom DBRs would eliminate the diffraction loss, leading to higher differential efficiency and lower threshold current provided surface roughness is sufficiently small.

Light-current-voltage characteristics for Samples A and B are shown in Fig. 3. Significantly higher differential efficiency ( $\eta_d$ ) is clearly seen with Sample B, attributed from the much lower optical loss. The inset of Fig. 3 shows the lasing spectrum at  $\sim 1538\ \text{nm}$ . The lack of an optical aperture results in a multimode spectrum. Threshold voltages were 4.56 V and 4.57 V for Samples A and B, respectively. This is only 0.6 V higher than the net active region junction voltage of 4 V ( $5 \times 0.8\ \text{V}$ ). Separately grown TJ voltages were measured to be around 80 mV at  $1\ \text{kA}/\text{cm}^2$ . Figure 4 shows a plot of differential quantum efficiencies versus pillar diameters. Greater than 100% efficiencies, only possible with cascaded active regions, are seen for a range of device sizes for Sample B. A device with a  $31\ \mu\text{m}$  pillar diameter showed 122% efficiency. It can also be mentioned that while  $\eta_d$  sub-linearly decreased for Sample A, it remained constant for

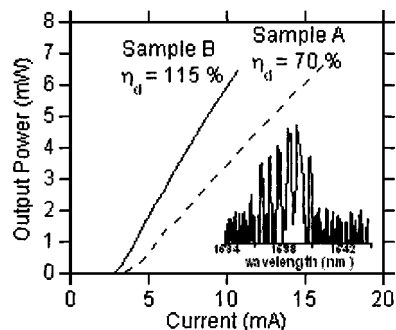


FIG. 3. Light-current-voltage plot of Samples A and B under pulsed operation at  $20\ ^\circ\text{C}$ .

Sample B until the device size became smaller than  $20\ \mu\text{m}$ . At this point, sidewall scattering becomes significant and  $\eta_d$  starts to decrease.

While the diffraction-free structure of Sample B is attractive, Sample A may be more practical because heat can dissipate more effectively in Sample A. It is possible to reduce diffraction loss of unguided DBR by using less number of periods. To investigate this, numerical simulation of the diffraction loss was carried out by Fourier decomposition method described in Babic *et al.*<sup>8</sup> First, the fundamental mode of a MAR VCSEL,  $\psi_I$ , was calculated by solving a two-dimensional scalar wave equation. The field profile is then decomposed into its plane-wave Fourier components which is then multiplied by bottom DBR's angular spectrum. Finally, an overlap integral of the reflected mode,  $\psi_R$ , and  $\psi_I$  was calculated

$$\kappa = \frac{\int d^2r \psi_R \cdot \psi_I^*}{\int d^2r \psi_I \cdot \psi_I^*}. \quad (1)$$

The diffraction loss can then be calculated from  $\delta = 1 - \kappa^*$ . Figure 5 shows the diffraction loss versus the number of DBR pairs for a pillar diameter of  $8\ \mu\text{m}$  with corresponding reflectivity shown on the top  $x$  axis. The reduction of the diffraction loss is clearly seen for lower reflective DBRs. However, ordinary single-stage VCSELs would severely suffer an increase of the threshold gain and current if the output DBR reflectivity is reduced. On the other hand, in bipolar-cascade devices, multiple-active stages can compensate for the increased mirror loss to keep the threshold gain within each QWs approximately the same.

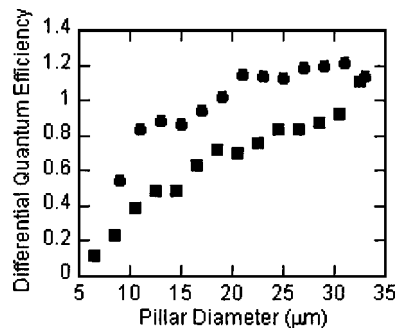


FIG. 4. Differential quantum efficiency vs pillar diameter for Sample A (square) and Sample B (circle).

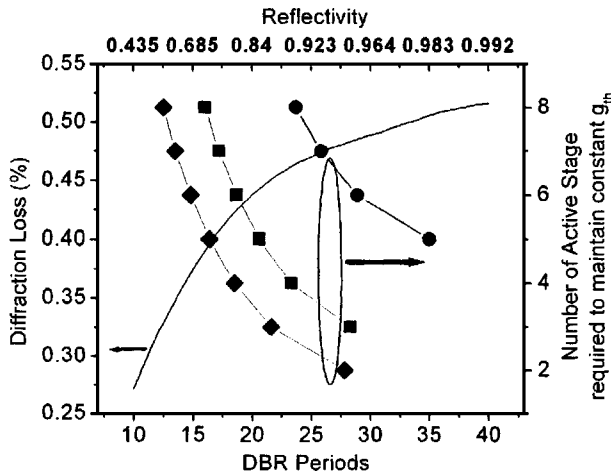


FIG. 5. Simulated diffraction loss for an 8  $\mu\text{m}$  pillar vs number of DBR periods, with the top axis indicating the corresponding reflectivity. The number of active stages required to maintain constant threshold gains of 414  $\text{cm}^{-1}$  (circles), 800  $\text{cm}^{-1}$  (squares), and 1200  $\text{cm}^{-1}$  (diamonds) is also plotted as a function of the number of DBR periods and reflectivity.

The threshold gain within the QWs of bipolar-cascade VCSELs was derived by Knodl *et al.*<sup>6</sup> and shown below as a reference

$$g_{\text{th}} \approx \frac{\tilde{g}_{\text{th}}}{N_a} + \frac{\alpha \Delta L}{N_a \Gamma d} - \frac{\ln \sqrt{\xi}}{N_a \Gamma d}, \quad (2)$$

where  $\tilde{g}_{\text{th}}$  is the threshold gain of a single-stage VCSEL with an active thickness of  $d$ ,  $N_a$  is the number of stages,  $\alpha$  is the absorption coefficient in the extended active region of  $\Delta L$ , and  $\Gamma$  is the confinement factor. Output mirror reflectivity of cascaded devices,  $R_o$  were related to single-stage one,  $\tilde{R}_o$  by  $R_o = \xi \tilde{R}_o$ . Using Eq. (2), the number of active stages required to maintain a constant threshold gain for different reflectivity was calculated and shown also in Fig. 5. For  $g_{\text{th}} = 1200 \text{ cm}^{-1}$  (diamonds), more than 20% reduction of dif-

fraction loss is possible by reducing the number of DBR periods from 28 to 15 by changing the number of stages from 2 to 6.

In this letter, we presented a 1550 nm five-stage MAR-VCSEL with greater than 120% efficiency using improved DBRs and TJ voltages. We also have experimentally demonstrated that the diffraction loss has a significant impact on device performance for a broad area air-post VCSEL structure. The increased gain of a MAR-VCSEL can enable a reduction in diffraction loss by the use of fewer periods in the DBRs without suffering the increase of threshold gain. Equations (1) and (2) can be used to estimate diffraction loss and the optimal number of active stage as illustrated in Fig. 5.

This project was funded by ARO through UCSD subcontract and CHIPS through DARPA.

- <sup>1</sup>A. Karim, J. Piprek, P. Abraham, D. Lofgreen, Y. J. Chiu, and J. E. Bowers, *IEEE J. Sel. Top. Quantum Electron.* **7**, 178 (2001).
- <sup>2</sup>S. Nakagawa, E. Hall, G. Almuneau, J. K. Kim, D. A. Buell, H. Kroemer, and L. A. Coldren, *IEEE J. Sel. Top. Quantum Electron.* **7**, 224 (2001).
- <sup>3</sup>C. K. Lin, D. P. Bour, Z. Jintian, W. H. Perez, M. H. Leary, A. Tandon, S. W. Corzine, and M. R. T. Tan, *IEEE J. Sel. Top. Quantum Electron.* **9**, 1415 (2003).
- <sup>4</sup>J. Boucart, C. Starck, F. Gaborit, A. Plais, N. Bouche, E. Derouin, L. Goldstein, C. Fortin, D. Carpentier, P. Salet, F. Brillouet, and J. Jacquet, *IEEE Photonics Technol. Lett.* **11**, 629 (1999).
- <sup>5</sup>J. K. Kim, S. Nakagawa, E. Hall, and L. A. Coldren, *Appl. Phys. Lett.* **77**, 3137 (2000).
- <sup>6</sup>T. Knodl, M. Golling, A. Straub, R. Jager, R. Michalzik, and K. J. Ebeling, *IEEE J. Sel. Top. Quantum Electron.* **9**, 1406 (2003).
- <sup>7</sup>P. M. Mayer, F. Rana, and R. J. Ram, *Appl. Phys. Lett.* **82**, 689 (2003).
- <sup>8</sup>D. I. Babic, Y. Chung, N. Dagli, and J. E. Bowers, *IEEE J. Sel. Top. Quantum Electron.* **29**, 1950 (1993).
- <sup>9</sup>M. J. Noble, P. Sotirelis, J. A. Lott, and J. P. Loehr, *SPIE-Int. Soc. Opt. Eng.* **3944**, 252 (2000).
- <sup>10</sup>R. Shau, M. Ortsiefer, J. Roskopf, G. Bohm, F. Kohler, and M.-C. Amann, *Electron. Lett.* **37**, 1295 (2001).
- <sup>11</sup>M. Miller, M. Grabherr, R. Jager, and K. J. Ebeling, *IEEE Photonics Technol. Lett.* **13**, 173 (2001).